

Andreas W. Reske
Harald Busse
Marcelo B. P. Amato
Matthias Jaekel
Thomas Kahn
Peter Schwarzkopf
Dierk Schreiter
Udo Gottschaldt
Matthias Seiwerts

Image reconstruction affects computer tomographic assessment of lung hyperinflation

Received: 4 September 2007
Accepted: 17 May 2008
Published online: 8 June 2008
© Springer-Verlag 2008

This work was supported by institutional sources and in part by funding to Andreas Reske from the German Interdisciplinary Association of Critical Care Medicine.

A. W. Reske · U. Gottschaldt
Department of Anesthesiology and
Intensive Care Medicine, University
Hospital Leipzig, Leipzig, Germany

H. Busse · M. Jaekel · T. Kahn ·
P. Schwarzkopf · M. Seiwerts
Department of Diagnostic and
Interventional Radiology, University
Hospital Leipzig, Leipzig, Germany

M. B. P. Amato
Respiratory ICU, Hospital das Clínicas,
Pulmonary Division, University of São
Paulo, Sao Paulo, Brazil

D. Schreiter
Surgical Intensive Care Unit, University
Hospital Leipzig, Leipzig, Germany

A. W. Reske (✉)
Klinik und Poliklinik fuer Anaesthesiologie
und Intensivtherapie, Universitaetsklinikum
Leipzig, Liebigstrasse 20, 04103 Leipzig,
Germany
e-mail: andreas.reske@medizin.
uni-leipzig.de
Tel.: +49-176-14455000
Fax: +49-341-9717709

Abstract Objectives: Lung hyperinflation may be assessed by computed tomography (CT). As shown for patients with emphysema, however, CT image reconstruction affects quantification of hyperinflation. We studied the impact of reconstruction parameters on hyperinflation measurements in mechanically ventilated (MV) patients. **Design:** Observational analysis. **Setting:** A University hospital-affiliated research Unit. **Patients:** The patients were MV patients with injured ($n = 5$) or normal lungs ($n = 6$), and spontaneously breathing patients ($n = 5$). **Interventions:** None. **Measurements and results:** Eight image series involving 3, 5, 7, and 10 mm slices and standard and sharp filters were reconstructed from identical CT raw data. Hyperinflated (V_{hyper}), normally (V_{normal}), poorly (V_{poor}), and nonaerated (V_{non}) volumes were calculated by densitometry as percentage of total lung volume (V_{total}). V_{hyper} obtained with the sharp filter systematically exceeded that with the standard filter showing a median (interquartile range) increment of 138 (62–272) ml corresponding to approximately 4% of V_{total} . In contrast, sharp filtering

minimally affected the other subvolumes (V_{normal} , V_{poor} , V_{non} , and V_{total}). Decreasing slice thickness also increased V_{hyper} significantly. When changing from 10 to 3 mm thickness, V_{hyper} increased by a median value of 107 (49–252) ml in parallel with a small and inconsistent increment in V_{non} of 12 (7–16) ml. **Conclusions:** Reconstruction parameters significantly affect quantitative CT assessment of V_{hyper} in MV patients. Our observations suggest that sharp filters are inappropriate for this purpose. Thin slices combined with standard filters and more appropriate thresholds (e.g., –950 HU in normal lungs) might improve the detection of V_{hyper} . Different studies on V_{hyper} can only be compared if identical reconstruction parameters were used.

Keywords Lung hyperinflation · Acute respiratory failure · Mechanical ventilation · Lung volume measurements · Computed tomography

Introduction

Computed tomographic (CT) densitometry of the lung is a reliable method to detect pathological changes in lung aeration. The quasi-linear relationship between X-ray attenuation and soft tissue density enables quantification of the amount of gas per unit of tissue with remarkable precision [1].

As both extremes of lung aeration, collapse and hyperinflation, seem to contribute to ventilator-associated lung injury [2], many studies of mechanically ventilated patients have used CT to quantify such pathological lung conditions. For instance, by treating voxels pertaining to a specific range of aeration as an independent lung compartment, researchers have calculated the size of the nonaerated or hyperinflated subvolumes. Recently, controversial conclusions about the physiological effects of positive end-expiratory pressure (PEEP) and tidal volumes have been drawn from such results [3–15]. These densitometric measurements, however, depend on the technical parameters of the CT scan protocol itself and the image reconstruction algorithms applied [1, 4, 5, 14, 16–32]. Not often recalled, image reconstruction parameters have been shown to affect the calculated volume of the emphysematous lung compartment, and thresholds for emphysema quantification also depend on the reconstruction details [16–29].

We hypothesized that CT image reconstruction could similarly affect the measurement of hyperinflation in mechanically ventilated patients to such an extent that clinical judgment might be influenced significantly. Therefore, we analyzed the influence of two parameters, slice thickness and reconstruction filter, on hyperinflation in mechanically ventilated patients with or without lung injury. For comparison, we also investigated a group of spontaneously breathing patients, with normal lungs.

Materials and methods

Patients

The institutional ethics committee approved this study. Because the observational analysis of CT data did not require patient manipulation, the need for informed consent was waived. Patients with routine thoracic CT scans were retrospectively assigned to three groups: (1) *Acute respiratory failure (ARF)*: five polytrauma patients presenting with pulmonary infiltrates and impaired oxygenation; (2) *normal-ventilated*: six polytrauma patients with normal lung CT; (3) *normal-spontaneous*: five spontaneously breathing patients with normal lungs. Patients with pneumothoraces, known emphysematous lung disease, or significant respiratory artifacts in CT images were not included. Physiological data was

gathered from the patient data management system of our ICU.

All patients with polytrauma were treated according to institutional guidelines, including a whole-body CT scan with contrast medium [8]. Initial pressure-controlled mechanical ventilation (Oxylog 3000, Dräger, Lübeck, Germany) during primary resuscitation and CT scanning was standardized, and it included the following ventilator settings: tidal volume of 6–8 ml/kg estimated body weight (Broca formula), a respiratory rate of 20 min⁻¹, and PEEP of 10 cm H₂O unless higher PEEP had been applied before CT.

CT scanning and image reconstruction

Each patient had one single multislice helical CT scan (Somatom Volume Zoom, Siemens, Erlangen, Germany) using the following protocol: 120 kV tube voltage, tube current between 100 and 200 mAs, 4 × 2.5 mm collimation, pitch 1.1, and 0.5 s gantry rotation. Spontaneously breathing patients were scanned during breath hold after full inspiration and mechanically ventilated patients were scanned during uninterrupted ventilation. Since landmark studies estimating thresholds for separating hyperinflation from normally aerated lung were performed using contrast medium, we included only patients who had received 120 ml of Iopamidol (Schering AG, Berlin, Germany) [4, 33]. Autocalibration for air, and calibration using the manufacturer's standard phantom were performed daily and weekly, respectively.

From identical CT raw data, predefined image series covering the entire lung were reconstructed using an identical field of view and contiguous slices of effective thickness 3, 5, 7, and 10 mm. During routine clinical imaging, two reconstruction filters—a standard (manufacturer's designation: B35f, medium heart) and a sharp body filter (B60f, medium sharp)—were applied (Table 1). The assignments of standard and sharp were made according to Boedeker et al. [22]. *Sample volumes* were calculated using the theoretical parameters of the filters provided by the manufacturer [20]. When referring to a particular reconstruction method, the abbreviation “filter_thickness” is used. For example, std_10 denotes reconstruction with standard filter and 10 mm slice thickness (Table 1).

Image segmentation

Image segmentation was performed on a 3D workstation (Virtuoso, Siemens) and involved a threshold-based region growing algorithm followed by interactive manual refinement [19]. Major pulmonary vessels, trachea, and main bronchi were excluded. All CT images were analyzed by two independent observers. Lung subvolumes

Table 1 Details of the CT image series

Reconstruction method ID label	Slice thickness (mm)	Reconstruction filter (manufacturer's ID)	Sample volume (mm ³)
std_10	10	B35f	16.0
std_7	7	B35f	11.2
std_5	5	B35f	8.0
std_3	3	B35f	4.8
shp_10	10	B60f	7.8
shp_7	7	B60f	5.5
shp_5	5	B60f	3.9
shp_3	3	B60f	2.4

Image reconstruction from identical raw data was performed with a standard (std) and a sharp body reconstruction filter (shp)

Sample volumes were calculated according to Kemerink et al. [20]

were classified as hyperinflated (V_{hyper} , $-1,000$ to -901 HU), normally aerated (V_{normal} , -900 to -501 HU), poorly aerated (V_{poorly} , -500 to -101 HU) and nonaerated (V_{non} , -100 to $+100$ HU), and calculated as the sum over all voxels in the respective HU ranges [4, 10, 13, 14]. The sum of these subvolumes was defined as V_{total} . The subvolume of voxels within the $-1,000$ to -950 HU range was also calculated. In addition to absolute values, all subvolumes were calculated as percentage of V_{total} .

Statistical analysis

Data are presented as median (interquartile range). Volumes were rounded to the nearest milliliter. Age, body mass index, and PEEP differences were evaluated by Kruskal–Wallis and Mann–Whitney tests, respectively. Bland–Altman plots were used to evaluate the agreement of relative subvolumes obtained in 10 mm slices combined with different filters. The interobserver agreement of absolute subvolume readings was also assessed by Bland–Altman's technique. In these plots, the mean volume obtained by two different reconstruction methods or observers, respectively, was plotted on the x axis. The difference between these values was calculated as percentage of the mean, and plotted on the y axis [34, 35]. To analyze the influence of thickness and filter on relative V_{hyper} and V_{non} by repeated measures ANOVA, the respective values from all patients were transformed (V_{hyper} : square-root, V_{non} : natural logarithm) to conform to normality assumptions and homoscedasticity. Histograms, and Shapiro–Wilk and Levene tests were used to confirm the normal distribution. Filter and thickness were used as within-subject, and group (i.e., ARF, normal-ventilated and normal-spontaneous) as between-subject factor. Interaction terms were also included in the model. Bonferroni t test was used for pairwise post-hoc testing. Because of the limited number of patients in each group, further intergroup comparison was omitted. Significance was set at $P < 0.05$. Statistical

analyses were performed with SPSS 11.0 (SPSS GmbH, Munich, Germany).

Results

Patient characteristics are given in Table 2. Intergroup differences in age ($P = 0.67$) and body mass index ($P = 0.60$) were not significant. PEEP levels during CT did not differ between ARF and normal-ventilated patients ($P = 1.0$). Relative and absolute CT subvolumes for all groups are given in Tables 3 and 4, respectively.

For all patients, V_{hyper} varied significantly with every change of reconstruction method (all P values ≤ 0.001 ; Tables 3, 4; Figs. 1, 2). Extreme values for V_{hyper} were observed for std_10 and shp_3, with median values over all patients of 0.3 (0–1.3)% and 8.8 (4–13.1)%, respectively. For ARF, normal-ventilated, and normal-spontaneous patients, the median absolute difference in V_{hyper} between shp_3 and std_10 was 150 (61–208) ml, 426 (146–541) ml, and 372 (332–461) ml, respectively.

V_{hyper} obtained with the sharp filter systematically exceeded that with the standard filter showing a median increment of 138 (62–272) ml corresponding to approximately 4% of V_{total} (Figs. 2, 3). The influence of both, thickness and filter on V_{hyper} was statistically significant (ANOVA P values < 0.001 for both relative and absolute values). Thinner slices caused more pronounced increments if combined with sharp filters ($P < 0.001$ for the interaction term).

The impact of filter on all other subvolumes (V_{non} , V_{normal} , and V_{poor}) was much smaller than that on V_{hyper} (Tables 3, 4; Figs. 2, 3). Although there was a slight reduction in V_{non} associated with the sharp filter in ARF patients (Figs. 2, 3), the overall effect of filter on V_{non} was not significant ($P = 0.35$).

Independent of the filter used, V_{hyper} increased markedly with decreasing thickness in all patients ($P < 0.001$; Tables 3, 4; Figs. 1, 2). Decreasing thickness also caused a small but statistically significant ($P < 0.001$) increment of V_{non} (1% of V_{total}). Nevertheless, the increment of V_{hyper} amounted to 107 (49–252) ml when changing from 10 to 3 mm slices, whereas the corresponding median increment of V_{non} was only 12 (7–16) ml. Moreover, the effect on V_{non} was consistent only in normal-ventilated and normal-spontaneous patients (Tables 3, 4; Fig. 2). In ARF patients, decreasing thickness slightly increased V_{non} only if combined with the standard filter.

Use of a more conservative threshold (-950 instead of -900 HU) significantly decreased V_{hyper} in 3 mm slices for both filters ($P < 0.001$). V_{hyper} in std_3 yielded 0 (0–0.1)%, 0.1 (0–0.2)%, and 0.1 (0–0.2)% for ARF, normal-ventilated, and normal-spontaneous patients, respectively. In shp_3, the corresponding values were 0.6 (0.4–1.3)%, 2.1 (0.5–3.2)%, and 1.7 (1.0–2.9)%.

Table 2 Patient data

Group	Patient	Age, Sex	Indication for CT	Pulmonary findings in CT	Height (cm), Weight (kg)	BMI	Smoker (pack-years)	PEEP, PIP (cm H ₂ O)	PaO ₂ /FiO ₂ (mmHg)	PaCO ₂ (mmHg)
<i>ARF</i>	A1	54, M	Polytrauma	PC, atelectasis	156, 80	33	No	10, 31	112	38.9
	A2	43, M	Polytrauma	PC, atelectasis	186, 98	28	No	10, 32	65	54.2
	A3	19, M	Polytrauma	PC, atelectasis	170, 65	22	Yes, 1	12, –	285	34.0
	A4	19, M	Polytrauma	PC, PH, atelectasis	170, 60	21	Yes, 1	10, 25	278	37.9
	A5	40, M	Polytrauma	PC, atelectasis	175, 88	29	No	No MV	242	40.6
<i>Normal-ventilated</i>	V1	24, F	Polytrauma	Normal	162, 75	29	Yes, 1	10, 24	543	32.9
	V2	24, M	Polytrauma	Normal	165, 75	28	Yes, 15	10, 25	350	40.1
	V3	20, M	Polytrauma	Normal	180, 80	25	Yes, 1	10, 26	571	36.5
	V4	29, M	Polytrauma	Normal	190, 100	28	Yes, 6	10, 26	502	32.0
	V5	19, M	Polytrauma	Normal	173, 80	27	No	10, 25	525	45.8
	V6	21, M	Polytrauma	Normal	175, 70	23	Yes, 2	10, 21	608	30.6
<i>Normal-spontaneous</i>	S1	19, M	Polytrauma	Normal	191, 75	21	Yes, 1	No MV	–	–
	S2	62, F	Screening	Normal	158, 77	31	Yes, 17	No MV	–	–
	S3	45, F	Suspected PE	Normal	175, 85	28	No	No MV	–	–
	S4	27, F	Polytrauma	Normal	168, 49	17	No	No MV	–	–
	S5	20, M	Polytrauma	Normal	175, 72	24	No	No MV	–	–

Dash symbol indicates missing data

Screening, patient S2 underwent CT for cancer follow-up

BMI body mass index, *MV* mechanical ventilation, *PEEP* positive end-expiratory pressure at the time of CT (in cm H₂O), *PIP* peak inspiratory pressure, *PaO₂/FiO₂* ratio of the partial pressure of

arterial oxygen to the fraction of inspired oxygen, *PaCO₂* partial pressure of arterial carbon dioxide, *M* male, *F* female, *PC* pulmonary contusion, *PH* pulmonary hemorrhage, *PE* pulmonary embolism

Table 3 Influence of CT image reconstruction on relative pulmonary subvolumes

	Recon	V _{total} (ml)	V _{hyper} (%)	V _{normal} (%)	V _{poor} (%)	V _{non} (%)	
<i>ARF</i>	std 10	3,646 (2,948–4,023)	0 (0–0)	61 (44–82)	22 (13–27)	17 (4–29)	
	std 7.0	3,652 (2,937–4,039)	0 (0–0)	62 (47–82)	17 (13–23)	18 (4–29)	
	std 5.0	3,647 (2,918–4,025)	0 (0–1)	63 (46–83)	18 (12–24)	18 (5–29)	
	std 3.0	3,647 (2,918–4,032)	0 (0–1)	62 (47–82)	17 (13–23)	18 (5–29)	
	shp 10	3,581 (2,799–3,951)	1 (0–2)	60 (45–82)	22 (13–28)	15 (4–26)	
	shp 7.0	3,563 (2,765–3,946)	1 (1–3)	61 (47–82)	19 (12–26)	15 (4–26)	
	shp 5.0	3,547 (2,731–3,894)	2 (1–5)	61 (48–81)	18 (12–25)	15 (4–26)	
	shp 3.0	3,546 (2,694–3,877)	4 (2–7)	60 (48–79)	17 (12–24)	15 (4–25)	
	<i>Normal-ventilated</i>	std 10	4,226 (3,672–4,735)	1 (0–2)	87 (84–89)	11 (8–13)	0 (0–2)
		std 7.0	4,222 (3,663–4,729)	1 (0–3)	87 (85–89)	10 (8–12)	1 (0–2)
std 5.0		4,215 (3,650–4,721)	2 (0–4)	87 (85–89)	10 (7–11)	1 (0–2)	
std 3.0		4,225 (3,654–4,733)	3 (1–6)	86 (83–88)	10 (8–11)	1 (1–3)	
shp 10		4,143 (3,620–4,636)	4 (1–7)	84 (81–87)	11 (8–12)	0 (0–2)	
shp 7.0		4,142 (3,608–4,634)	6 (2–9)	84 (79–86)	10 (7–11)	1 (0–2)	
shp 5.0		4,117 (3,593–4,612)	8 (2–12)	83 (78–85)	9 (7–11)	1 (1–2)	
shp 3.0		4,109 (3,589–4,590)	11 (4–15)	80 (74–83)	9 (7–11)	1 (1–2)	
<i>Normal-spontaneous</i>		std 10	4,260 (3,466–4,911)	1 (0–2)	90 (88–91)	8 (8–11)	0 (0–0)
		std 7.0	4,248 (3,465–4,902)	1 (0–2)	90 (88–91)	7 (7–11)	0 (0–1)
	std 5.0	4,231 (3,454–4,896)	2 (1–3)	90 (88–91)	7 (7–10)	0 (0–1)	
	std 3.0	4,220 (3,459–4,895)	4 (1–4)	88 (87–90)	7 (7–10)	0 (0–1)	
	shp 10	4,147 (3,387–4,850)	4 (2–7)	87 (84–90)	7 (7–10)	0 (0–0)	
	shp 7.0	4,134 (3,375–4,835)	6 (3–9)	86 (83–89)	7 (7–9)	0 (0–1)	
	shp 5.0	4,099 (3,352–4,810)	8 (5–11)	85 (81–88)	7 (6–9)	0 (0–1)	
	shp 3.0	4,081 (3,339–4,796)	10 (8–15)	81 (77–85)	7 (6–9)	1 (0–1)	

Influence of CT image reconstruction method on the relative subvolumes V_{hyper}, V_{normal}, V_{poor}, and V_{non}, which were calculated as percentage of the total lung volume and rounded to the nearest integer

The absolute V_{total} is given to allow approximate calculation of the absolute subvolumes

All values are median (interquartile range)

Recon reconstruction method, *ml* milliliters

Table 4 Influence of CT image reconstruction on absolute pulmonary subvolumes

	Recon	V_{hyper} (ml)	V_{normal} (ml)	V_{poor} (ml)	V_{non} (ml)	
<i>ARF</i>	std 10	1 (1–5)	1,959 (1,493–3,120)	654 (485–1,017)	536 (164–934)	
	std 7.0	3 (2–11)	2,001 (1,545–3,147)	614 (453–945)	551 (165–949)	
	std 5.0	6 (5–21)	2,006 (1,574–3,151)	577 (433–891)	556 (170–948)	
	std 3.0	18 (10–42)	1,988 (1,588–3,138)	556 (428–878)	575 (171–950)	
	shp 10	29 (13–67)	1,839 (1,483–3,067)	636 (464–994)	459 (143–829)	
	shp 7.0	53 (23–100)	1,870 (1,511–3,064)	582 (429–916)	462 (144–823)	
	shp 5.0	87 (37–146)	1,896 (1,498–3,029)	555 (407–855)	451 (144–788)	
	shp 3.0	151 (62–214)	1,895 (1,461–2,950)	505 (405–847)	443 (149–760)	
	<i>Normal-ventilated</i>	std 10	47 (4–104)	3,662 (3,178–4,250)	428 (389–476)	19 (16–69)
		std 7.0	62 (8–139)	3,654 (3,201–4,241)	400 (369–439)	22 (18–78)
std 5.0		89 (14–184)	3,633 (3,207–4,205)	374 (355–412)	25 (21–84)	
std 3.0		129 (25–256)	3,574 (3,192–4,144)	381 (357–416)	30 (27–94)	
shp 10		185 (36–332)	3,461 (3,117–3,920)	406 (357–452)	20 (15–68)	
shp 7.0		254 (56–415)	3,437 (3,078–3,846)	375 (336–412)	24 (19–74)	
shp 5.0		353 (89–510)	3,380 (3,005–3,737)	349 (317–382)	26 (23–77)	
shp 3.0		483 (150–629)	3,277 (2,880–3,574)	348 (326–382)	33 (30–83)	
<i>Normal-spontaneous</i>		std 10	27 (11–64)	3,733 (3,092–4,473)	408 (296–458)	9 (5–19)
		std 7.0	51 (20–78)	3,743 (3,092–4,474)	386 (273–430)	12 (7–21)
	std 5.0	80 (33–108)	3,732 (3,071–4,453)	360 (258–415)	16 (8–25)	
	std 3.0	133 (62–161)	3,696 (3,008–4,409)	364 (264–412)	20 (12–30)	
	shp 10	155 (83–250)	3,601 (2,839–4,354)	378 (277–412)	10 (6–18)	
	shp 7.0	218 (135–314)	3,563 (2,787–4,314)	343 (250–380)	12 (7–21)	
	shp 5.0	299 (210–401)	3,476 (2,701–4,230)	312 (228–354)	17 (10–25)	
	shp 3.0	413 (342–518)	3,319 (2,573–4,084)	313 (228–350)	22 (15–32)	

Influence of CT image reconstruction method on the absolute subvolumes V_{hyper} , V_{normal} , V_{poor} , and V_{non}

All values are median (interquartile range) and were rounded to the nearest milliliter

Recon reconstruction method, *ml* milliliters

V_{total} changed very little with the reconstruction method. For *ARF* patients, the median V_{total} over all reconstruction methods was 3,613 ml, showing a maximum relative variation of 1.9%. For *normal-ventilated* patients, the corresponding variation was 1.7% at 4,179 ml, and for *normal-spontaneous* patients, it was 2.5% at 4,184 ml.

The interobserver agreement was good for V_{hyper} , V_{normal} , and V_{poor} . The worse agreement of V_{non} readings resulted mainly from *normal-spontaneous* and *normal-ventilated* patients, in whom small absolute interobserver differences translated into considerable percentages. Interobserver bias (standard deviation) observed in the Bland–Altman analysis were -0.1 (1.5)%, 0.0 (0.1)%, -0.4 (2.2)%, and 1.1 (12.0)% for V_{hyper} , V_{normal} , V_{poor} , and V_{non} , respectively.

Discussion

Our work shows that the assessment of lung hyperinflation by CT densitometry is significantly affected by image reconstruction parameters. Estimates of V_{hyper} , a variable originally conceived to identify truly pathological conditions of hyperinflation, were significantly magnified by using either sharp reconstruction filters or thin slices. While such an observation has already been made for

spontaneously breathing patients with emphysema, this study confirmed the same also for mechanically ventilated patients with either acutely injured or normal lungs. The magnitude of these effects is certainly of clinical relevance, since the estimates of V_{hyper} differed by up to 400 ml depending on the settings employed.

As both extremes of lung aeration – deaeration and hyperinflation – play a role in the pathogenesis of ventilator-associated lung injury [2], V_{hyper} has frequently been assessed by CT to evaluate this known side effect of mechanical ventilation [3–15]. When 10 mm slices are analyzed, a -900 HU threshold has been suggested to assess V_{hyper} in mechanically ventilated patients, which is similar to the threshold for emphysema (i.e., -910 HU) [4, 33].

Recently, however, some authors suggested that the use of thinner slices would increase spatial resolution and improve the detection of V_{hyper} [5, 7, 14]. Accordingly, Vieira et al. demonstrated that V_{hyper} assessed with the -900 HU threshold in 1.5 mm slices significantly exceeded that of 10 mm slices, concluding that the true V_{hyper} caused by mechanical ventilation had thus far been underestimated due to *partial-volume-artifacts* [5].

Theoretically, the approach of reducing *partial-volume-artifacts* seems sound. Because of the finite spatial resolution of CT, the size of the scanned (sampled) elementary tissue volume usually exceeds the alveolar dimensions by far. This implies that, within an elementary

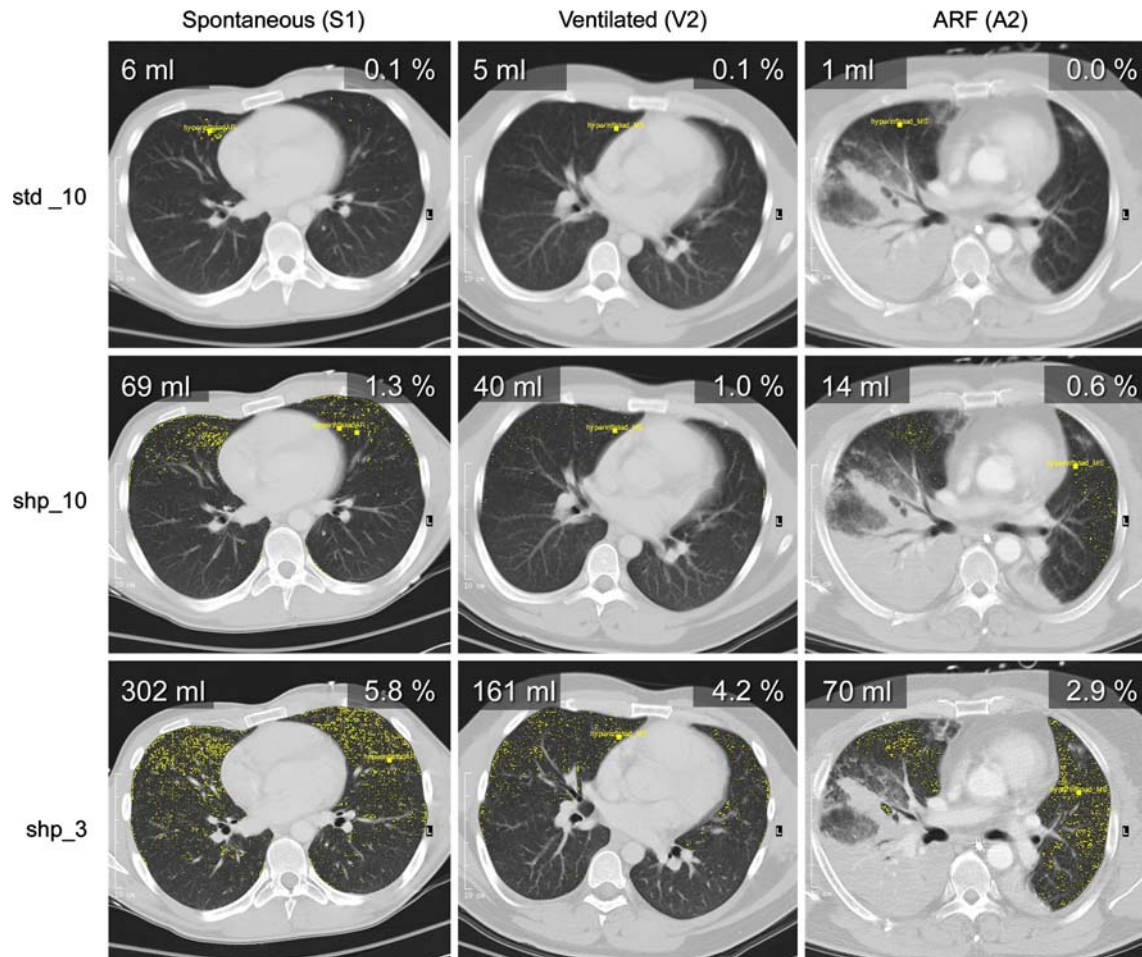


Fig. 1 CT images after segmentation of the lung for three representative patients and three image reconstruction methods: std_10, shp_10, and shp_3, respectively. Voxels contributing to V_{hyper} are marked yellow. Images are annotated with the absolute and relative V_{hyper} of the entire lung. Relative V_{hyper} are percentages

of V_{total} . Patient annotations (i.e., S1, V2, A2) correspond to Table 2. *Normal-spontaneous* patient S1 was scanned during end-inspiratory breath hold, *normal-ventilated* patient V2 and *ARF* patient A2 during uninterrupted mechanical ventilation

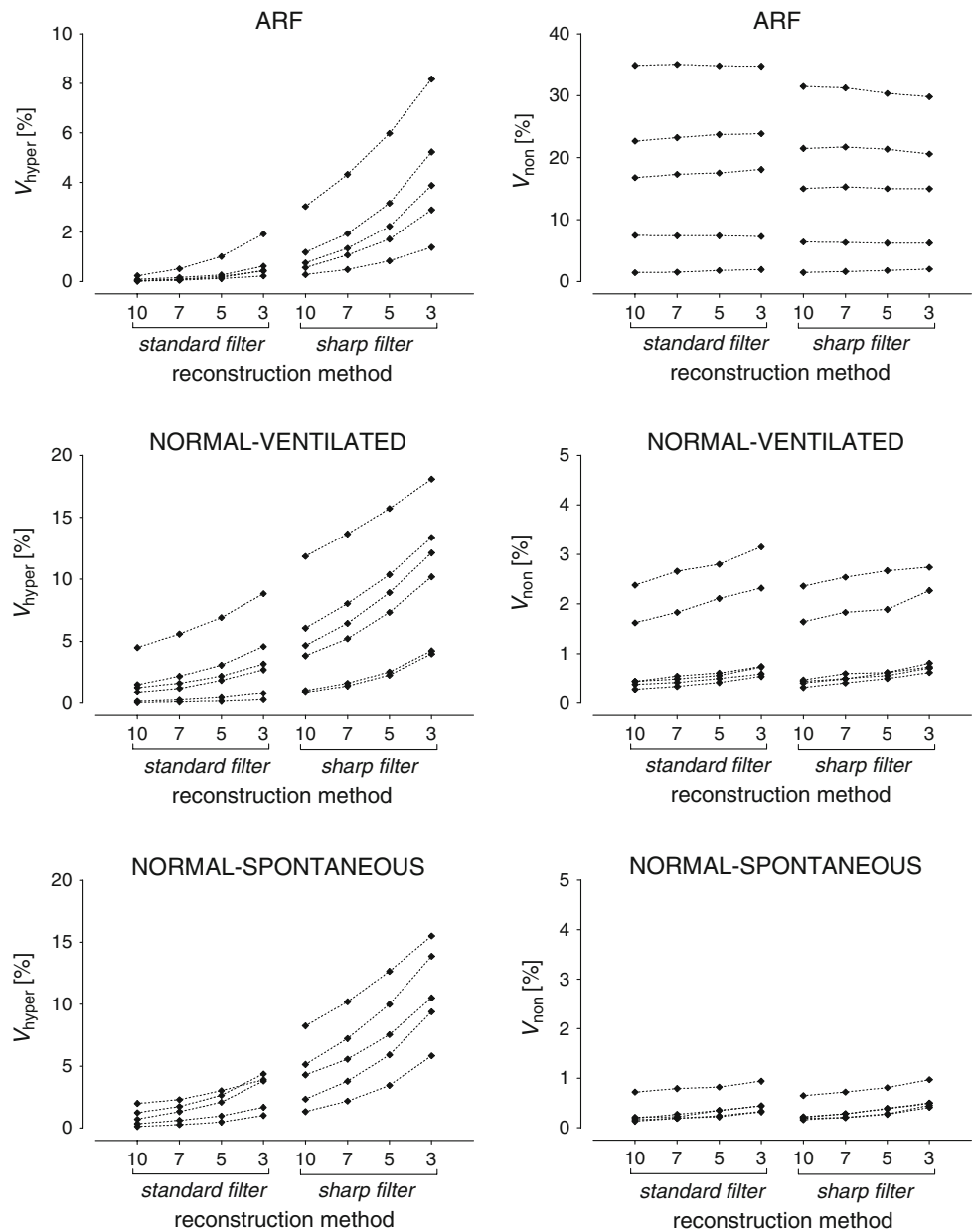
volume, a few collapsed or edematous alveoli could obscure the presence of many hyperinflated ones [5, 14]. This search for an improved spatial resolution, however, may be misleading under certain conditions. High-resolution CT (HRCT) is currently the method of choice for a *visual and qualitative assessment* of pathologic changes within the lung such as emphysema [30, 31], but the situation seems quite different for a *quantitative analysis* of V_{hyper} [19, 21, 27, 28, 36].

Even with HRCT, where thin slices are commonly used together with sharp filters, we are still far away from the spatial resolution required to display single (hyperinflated) alveoli [5, 20, 21, 31, 37]. Thus, instead of improving the detection of V_{hyper} , we may be trespassing the limits of density resolution of current CT technology. Kemerink et al. demonstrated that different reconstruction protocols may result in unacceptable differences in densitometric measurements, especially in heterogeneous foam-like

materials, and tried to overcome these limitations by introducing the concept of CT *sample volume* [20, 21]. While the voxel size represents an arbitrary volume within which the density information is displayed or interpolated, the *sample volume* is the minimum volume carrying truly independent information, not contaminated by neighborhood densities. It is the volume in a scanned section over which the X-ray attenuation is truly estimated and frequently encompasses a few contiguous voxels. According to Kemerink et al., comparability of densitometric results (and thus the threshold-based assessment of V_{hyper}) requires *sample volumes* above a critical value of 8 mm^3 [20, 21]. Discussion of the appropriateness of this value is beyond the scope of this work, but it is worth noting that we observed large increases in V_{hyper} when *sample volumes* were below 8 mm^3 .

Whenever spatial resolution is increased, for instance by using sharp filters and/or thin slices, the *sample volume*

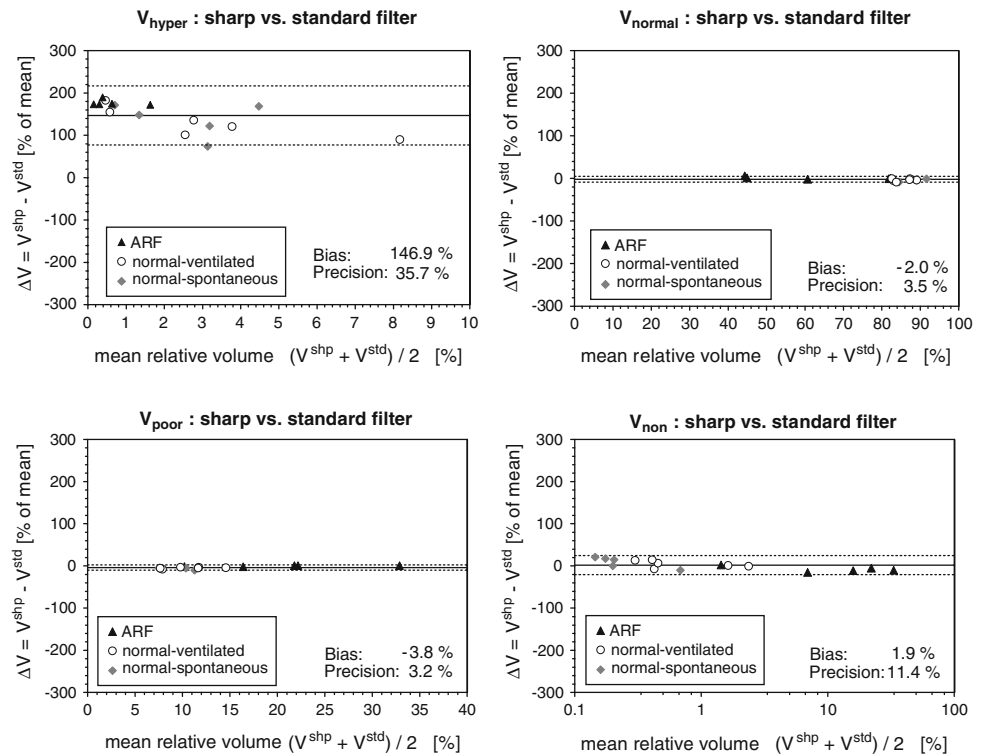
Fig. 2 Influence of image reconstruction on relative V_{hyper} (left column) and V_{non} (right column), respectively, for ARF, normal-spontaneous, and normal-ventilated patients. For each individual, the respective subvolume measured at slice thickness = 10, 7, 5, and 3 mm in combination with two different filters (i.e., standard and sharp filter) was calculated as percentage of V_{total} and plotted over the reconstruction method. Data points of individual patients were connected by dotted lines for better identification of individual changes



decreases and the histogram of CT numbers broadens due to an increased number of voxels with extreme values [19–23, 29, 31]. The key question is to what extent the broadened histogram and the associated increase in V_{hyper} is related to less *partial-volume-artifact* (i.e., better reflecting reality), and to what extent it is an artifact due to a too small *sample volume* (i.e., an increased amount of reconstruction noise). Important information to answer this question can be obtained from analysis of V_{non} —the subvolume at the other extreme of the histogram. According to Kemerink et al., the artifact caused by a too small *sample volume* produces a preferential overestimation of V_{hyper} with little effects on the other

compartments [20, 21]. In contrast, any decrease in *partial-volume-artifacts* should produce symmetric and similar effects in V_{non} , because vessels, bronchial walls, edematous or collapsed alveoli are reproduced with less contamination by surrounding lower density tissues [20, 21]. Although increments of V_{non} may not exactly mirror those of V_{hyper} , since this would require a mean lung density around -500 HU, the increments of V_{non} observed in our patients were much smaller than that expected. Thus, we must conclude that sharp filters were not appropriate for the assessment of V_{hyper} , especially in ARF patients: whatever the slice thickness, V_{hyper} from the sharp filter significantly exceeded the corresponding

Fig. 3 Influence of reconstruction filter on relative V_{hyper} , V_{normal} , V_{poor} , and V_{non} for a slice thickness of 10 mm. Bland–Altman plots show the agreement between the relative subvolumes derived from the standard (V^{std}) or sharp (V^{shp}) reconstruction filter. Relative subvolumes are percentages of V_{total} . Please note the logarithmic scale of the abscissa for V_{non}



V_{hyper} from the standard one, without any associated change in V_{non} (in fact there was a slight decrease).

A similar observation has been established for the quantification of emphysema, a condition where sharp filters are no longer recommended for the assessment of V_{hyper} , since they were shown to overestimate this subvolume [20–24, 26, 36].

In contrast to this straightforward conclusion about the inappropriateness of sharp filters, the results of our study are less conclusive regarding the possible artifact caused by thin slices. Both absolute V_{hyper} and V_{non} increased with decreasing thickness (Table 4). This was paralleled by a decrease in V_{poor} and particularly consistent for reconstructions using the standard filter. Such behavior is compatible with a reduction in *partial-volume-artifacts*, suggesting a true advantage of thinner slices. When V_{non} was expressed as percentage of V_{total} (Table 3), however, it remained almost unchanged (Fig. 2). Furthermore, the median relative variation of V_{non} in *normal-ventilated* and *normal-spontaneous* was only about 1%, corresponding to an absolute volume of approximately 10 ml. Since V_{non} is more susceptible to subjective segmentation errors than V_{hyper} , such a small increase in V_{non} may also be related to a higher rate of segmentation errors when analyzing a great number of thin slices. Nevertheless, our analyses suggest that thinner slices (especially in combination with standard filter) enable assessment of V_{hyper} with less influence of *partial-volume-artifacts*. However, further studies seem necessary to prove this conclusively for the

assessment of lung hyperinflation associated with mechanical ventilation.

Thin slices have been implemented in several protocols for the CT quantification of V_{hyper} in emphysema, asthma or interstitial lung disease. To avoid an overestimation of V_{hyper} , however, most of these studies used -950 HU or even lower thresholds to separate V_{hyper} from normal lung [16, 18, 24, 27, 28, 30–32, 36, 38, 39]. Accordingly, the authors were able to reduce *partial-volume-artifacts* without the associated overestimation of V_{hyper} . Unfortunately, this procedure has not been adopted in studies about mechanical ventilation, and this may explain the high values of V_{hyper} reported in subjects scanned at low transpulmonary pressures [5, 6, 9, 15]. In all these studies, thin slices were analyzed with the traditional -900 HU threshold, sometimes in combination with sharp filters. In this context, it is interesting to note the significant decrease in V_{hyper} in 3 mm slices observed in our study after applying the -950 HU threshold.

It is likely, however, that no single threshold for V_{hyper} is universally appropriate, even when using intermediate slice thicknesses in combination with soft or standard filters [26]. Thresholds will not only vary with patient-specific factors [16, 36], but also with the severity of the lung pathology [5]. A gold standard for measurement of V_{hyper} in mechanically ventilated patients is lacking, especially for conditions in which the average lung density is increased, such as acute lung injury. Finally, even if V_{hyper} assessed by threshold-based CT densitometry might

correlate with macroscopic and microscopic morphometry (as shown for emphysema [32, 33, 39]), it is still a challenge to understand how we could relate it to physiological indicators of alveolar hyperinflation such as functional dead-space [40], septal stress, or increased cytokine release [7, 41].

Some limitations of our retrospective study deserve attention. Although a fixed CT protocol was used for each group, different respiratory conditions (e.g., slightly different PEEP levels) may have resulted in uncontrolled lung volumes at which CT data were acquired. Also, age, body mass index, and smoking habits differed between groups. Finally, the radiation dose (current-time product) had been chosen by the CT technician according to indication for CT and patient factors and thus varied among our patients. All these factors may have biased intergroup comparisons of V_{hyper} , but not the within-patient assessments, which were the focus of this study. Finally, two outliers can be recognized in the V_{hyper} column of Fig. 2 (*ARF* and *normal-ventilated*). The lower radiation doses applied in these two patients (100 mAs) might be an explanation for the high values of V_{hyper} , although such an artifact seemed to be limited in previous

studies [30, 32]. Anyway, we tested the overall analysis without these two outliers. We found that the trend of increasing V_{hyper} with higher image resolution remained, suggesting that our conclusions are robust.

In conclusion, CT-based assessment of the hyperinflated lung volume in mechanically ventilated patients is significantly affected by image reconstruction parameters. Sharp filters overestimate this volume whatever slice thickness they are combined with. Thin slices used in combination with standard filters seem to reduce *partial-volume-artifacts* and may improve the assessment of hyperinflation. This approach, however, would require the definition and validation of new HU thresholds (e.g., -950 HU in normal lungs). Quantitative data of different studies can only be compared if identical reconstruction parameters were used and comprehensively specified.

Acknowledgments The authors would like to thank Dr. Stephan H. Böhm for critical review of the manuscript and Dr. Alexander Reske for his help with data collection. Moreover, we thank Mrs. Mariana Pereira de Melo and Mrs. Bettina Hentschel for statistical advice.

References

- Mull RT (1984) Mass estimates by computed tomography: physical density from CT numbers. *AJR Am J Roentgenol* 143:1101–1104
- Dos Santos CC, Slutsky AS (2000) Invited review: mechanisms of ventilator-induced lung injury: a perspective. *J Appl Physiol* 89:1645–1655
- Dambrosio M, Roupie E, Mollet JJ, Anglade MC, Vasile N, Lemaire F, Brochard L (1997) Effects of positive end-expiratory pressure and different tidal volumes on alveolar recruitment and hyperinflation. *Anesthesiology* 87:495–503
- Vieira SR, Puybasset L, Richecoeur J, Lu Q, Cluzel P, Gusman PB, Coriat P, Rouby JJ (1998) A lung computed tomographic assessment of positive end-expiratory pressure-induced lung overdistension. *Am J Respir Crit Care Med* 158:1571–1577
- Vieira SR, Nieszkowska A, Lu Q, Elman M, Sartorius A, Rouby JJ (2005) Low spatial resolution computed tomography underestimates lung overinflation resulting from positive pressure ventilation. *Crit Care Med* 33:741–749
- David M, Karmrodt J, Bletz C, David S, Herweling A, Kauczor HU, Markstaller K (2005) Analysis of atelectasis, ventilated, and hyperinflated lung during mechanical ventilation by dynamic CT. *Chest* 128:3757–3770
- Terragni PP, Rosboch G, Tealdi A, Corno E, Menaldo E, Davini O, Gandini G, Herrmann P, Mascia L, Quintel M, Slutsky AS, Gattinoni L, Ranieri VM (2007) Tidal hyperinflation during low tidal volume ventilation in acute respiratory distress syndrome. *Am J Respir Crit Care Med* 175:160–166
- Schreiter D, Reske A, Stichert B, Seiwerts M, Böhm SH, Kloeppe R, Josten C (2004) Alveolar recruitment in combination with sufficient positive end-expiratory pressure increases oxygenation and lung aeration in patients with severe chest trauma. *Crit Care Med* 32:968–975
- Carvalho AR, Jandre FC, Pino AV, Bozza FA, Saluh JI, Rodrigues R, Soares JH, Giannella-Neto A (2006) Effects of descending positive end-expiratory pressure on lung mechanics and aeration in healthy anaesthetized piglets. *Crit Care* 10:R122
- Malbouisson LM, Muller JC, Constantin JM, Lu Q, Puybasset L, Rouby JJ, CT Scan ARDS Study Group (2001) Computed tomography assessment of positive end-expiratory pressure-induced alveolar recruitment in patients with acute respiratory distress syndrome. *Am J Respir Crit Care Med* 163:1444–1450
- Suarez-Sipmann F, Böhm SH, Tusman G, Pesch T, Thamm O, Reissmann H, Reske A, Magnusson A, Hedenstierna G (2007) Use of dynamic compliance for open lung positive end-expiratory pressure titration in an experimental study. *Crit Care Med* 35:214–221
- Borges JB, Okamoto VN, Matos GFJ, Carameo MPR, Arantes PR, Barros F, Souza CE, Victorino JA, Kacmarek RM, Barbas CSV, Carvalho CRR, Amato MBP (2006) Reversibility of lung collapse and hypoxemia in early acute respiratory distress syndrome. *Am J Respir Crit Care Med* 174:268–278
- Gattinoni L, Caironi P, Cressoni M, Chiumello D, Ranieri VM, Quintel M, Russo S, Patroniti N, Cornejo R, Bugeo G (2006) Lung recruitment in patients with the acute respiratory distress syndrome. *N Engl J Med* 354:1775–1786

14. Gattinoni L, Caironi P, Pelosi P, Goodman LR (2001) What has computed tomography taught us about the acute respiratory distress syndrome? *Am J Respir Crit Care Med* 164:1701–1711
15. Albaiceta GM, Taboada F, Parra D, Luyando LH, Calvo J, Menendez R, Otero J (2004) Tomographic study of the inflection points of the pressure–volume curve in acute lung injury. *Am J Respir Crit Care Med* 170:1066–1072
16. Madani A, Keyzer C, Gevenois PA (2001) Quantitative computed tomography assessment of lung structure and function in pulmonary emphysema. *Eur Respir J* 18:720–730
17. Madani A, Keyzer C, Gevenois PA (2004) Computed tomography assessment of lung structure and function in pulmonary emphysema. *Eur Respir Mon* 30:145–160
18. Madani A, Zanen J, de Maertelaer V, Gevenois PA (2006) Pulmonary emphysema: objective quantification at multi-detector row CT—comparison with macroscopic and microscopic morphometry. *Radiology* 238:1036–1043
19. Stoel BC, Stolk J (2004) Optimization and standardization of lung densitometry in the assessment of pulmonary emphysema. *Invest Radiol* 39:681–688
20. Kemerink GJ, Kruize HH, Lamers RJ (1997) The CT's sample volume as an approximate, instrumental measure for density resolution in densitometry of the lung. *Med Phys* 24:1615–1620
21. Kemerink GJ, Kruize HH, Lamers RJ, van Engelshoven JM (1997) CT lung densitometry: dependence of CT number histograms on sample volume and consequences for scan protocol comparability. *J Comput Assist Tomogr* 21:948–954
22. Boedeker KL, McNitt-Gray MF, Rogers SR, Truong DA, Brown MS, Gjertson DW, Goldin JG (2004) Emphysema: effect of reconstruction algorithm on CT imaging measures. *Radiology* 232:295–301
23. Shaker SB, Dirksen A, Laursen LC, Maltbaek N, Christensen L, Sander U, Seersholm N, Skovgaard LT, Nielsen L, Kok-Jensen A (2004) Short-term reproducibility of computed tomography-based lung density measurements in alpha-1 antitrypsin deficiency and smokers with emphysema. *Acta Radiol* 45:424–430
24. Parr DG, Stoel BC, Stolk J, Nightingale PG, Stockley RA (2004) Influence of calibration on densitometric studies of emphysema progression using computed tomography. *Am J Respir Crit Care Med* 170:883–890
25. Newell JD Jr, Hogg JC, Snider GL (2004) Report of a workshop: quantitative computed tomography scanning in longitudinal studies of emphysema. *Eur Respir J* 23:769–775
26. Stoel BC, Bakker ME, Stolk J, Dirksen A, Stockley RA, Piitulainen E, Russi EW, Reiber JH (2004) Comparison of the sensitivities of 5 different computed tomography scanners for the assessment of the progression of pulmonary emphysema: a phantom study. *Invest Radiol* 39:1–7
27. Müller NL, Coxson H (2002) Chronic obstructive pulmonary disease. 4: imaging the lungs in patients with chronic obstructive pulmonary disease. *Thorax* 57:982–985
28. Hoffman EA, Reinhardt JM, Sonka M, Simon BA, Guo J, Saba O, Chon D, Samrah S, Shikata H, Tschirren J, Palagyi K, Beck KC, McLennan G (2003) Characterization of the interstitial lung diseases via density-based and texture-based analysis of computed tomography images of lung structure and function. *Acad Radiol* 10:1104–1118
29. Hoffman EA, Olson LE (1998) Characteristics of respiratory system complexity captured via X-ray computed tomography. In: Hlastala MP, Robertson HT (eds) *Complexity in structure and function of the lung*. Marcel Dekker, New York, pp 325–378
30. Zaporozhan J, Ley S, Weinheimer O, Eberhardt R, Tsakiris I, Noshi Y, Herth F, Kauczor HU (2006) Multi-detector CT of the chest: influence of dose onto quantitative evaluation of severe emphysema: a simulation study. *J Comput Assist Tomogr* 30:460–468
31. Zaporozhan J, Ley S, Eberhardt R, Weinheimer O, Ilyushenko S, Herth F, Kauczor HU (2005) Paired inspiratory/expiratory volumetric thin-slice CT scan for emphysema analysis: comparison of different quantitative evaluations and pulmonary function test. *Chest* 128:3212–3220
32. Madani A, De Maertelaer V, Zanen J, Gevenois PA (2007) Pulmonary emphysema: radiation dose and section thickness at multidetector CT quantification—comparison with macroscopic and microscopic morphometry. *Radiology* 243:250–257
33. Muller NL, Staples CA, Miller RR, Abboud RT (1988) “Density mask”. An objective method to quantitate emphysema using computed tomography. *Chest* 94:782–787
34. Bland JM, Altman DG (1986) Statistical methods for assessing agreement between two methods of clinical measurement. *Lancet* 1(8476):307–310
35. Dewitte K, Fierens C, Stöckl D, Thienpont LM (2002) Application of the Bland–Altman plot for interpretation of method-comparison studies: a critical investigation of its practice. *Clin Chem* 48:799–801
36. Marsh S, Aldington S, Williams MV, Nowitz MR, Kingzett-Taylor A, Weatherall M, Shirtcliffe PM, McNaughton AA, Pritchard A, Beasley R (2007) Utility of lung density measurements in the diagnosis of emphysema. *Respir Med* 101:1512–1520
37. Litzlbauer HD, Neuhaeuser C, Moell A, Greschus S, Breithecker A, Franke FE, Kummer W, Rau WS (2006) Three-dimensional imaging and morphometric analysis of alveolar tissue from microfocal X-ray-computed tomography. *Am J Physiol Lung Cell Mol Physiol* 291:L535–L545
38. Mitsunobu F, Ashida K, Hosaki Y, Tsugeno H, Okamoto M, Nishida N, Nagata T, Takata S, Tanizaki Y (2003) Decreased computed tomographic lung density during exacerbation of asthma. *Eur Respir J* 22:106–112
39. Gevenois PA, De Vuyst P, de Maertelaer V, Zanen J, Jacobovitz D, Cosio MG, Yernault JC (1996) Comparison of computed density and microscopic morphometry in pulmonary emphysema. *Am J Respir Crit Care Med* 154:187–192
40. Tusman G, Suarez-Sipmann F, Böhm SH, Pech T, Reissmann H, Meschino G, Scandurra A, Hedenstierna G (2006) Monitoring dead space during recruitment and PEEP titration in an experimental model. *Intensive Care Med* 32:1863–1871
41. Grasso S, Stripoli T, De Michele M, Bruno F, Moschetta M, Angelelli G, Munno I, Ruggiero V, Anaclerio R, Cafarelli A, Driessen B, Fiore T (2007) ARDSnet ventilatory protocol and alveolar hyperinflation: role of positive end-expiratory pressure. *Am J Respir Crit Care Med* 176:761–767